SEMI-AUTOMATED CSG MODEL-BASED BUILDING EXTRACTION FROM PHOTOGRAMMETRIC IMAGES

S. D. Wang [a], Y. H. Tseng [b]

Department of Geomatics, National Cheng Kung University, No. 1 University Road, Tainan 70101, TAIWAN
[a] Ph.D. Candidate, TEL: +886-6-2370876 ext.852, FAX: +886-6-2375764, E-Mail: sendo@sv.ncku.edu.tw
[b] Professor, TEL: +886-6-2757575 ext.63835, FAX: +886-6-2375764, E-Mail: tseng@mail.ncku.edu.tw

Commission III, WG III/4

KEY WORDS: Digital, Photogrammetry, Semi-automation, Building, Extraction, Three-dimensional, Modelling, Measurement

ABSTRACT:

Using pre-defined models to extract spatial information of the building, called *model-based building extraction*, has been considered as a convincible approach to improve the existing photogrammetric techniques. However, there is still a bottleneck on the practical efficiency and accuracy. This paper proposed a semi-automated approach to extracting buildings from multiple aerial images as well as close-range images by a tailored *least-squares model-image fitting* (LSMIF) algorithm. Compare to the floating mark which is used by conventional photogrammetric techniques, we proposed a naval measuring tool of "floating models" for building extraction. The floating model is an abstract representation of the real object, which can be a point, a line segment, a surface plane, or a volumetric model. Each floating model is associated with a set of pose parameters and a set of shape parameters. By fitting the model to images, these parameters will not only reveal the location of the building but also describe the shape of the building. The semi-automated strategy for building extraction includes following five steps: (1) manually select an appropriate model, (2) manually locate and adjust the model for approximate fitting, (3) automatically compute the optimal fitting, (4) manually edit, and (5) compose the fitted models according to the *Constructive Solid Geometry* (CSG). An *ad hoc* computer program which was developed to implementing the proposed semi-automated approach was tested by extracting 10 selected buildings around the NCKU campus. The accuracy achieved was evaluated by comparing the roof corner coordinates with manual measurements.

1. INTRODUCTION

In response to the development of 3D City Spatial Information Systems for urban planning and management, acquisition of 3D data of city objects has increasingly become an important topic. This tendency leads to intense research activities aiming for automated or semi-automated building extraction from digital aerial images in both the photogrammetry and the computer vision communities (Mohan and Nevatia, 1989, Braun *et al.*, 1995, Englert and Gülch, 1996, Lang and Förstner, 1996, Vosselman and Veldhuis, 1999, Grün, 2000). While the task of building extraction may differ in terms of image data type and scale, object complexity, required level of detail, and type of product, the common process sequence would be: detection, reconstruction, and attribution. Various approaches have been implemented with emphasis on more or less automation with respect to the process sequence.

Conventional photogrammetry concentrates on the accurate 3D coordinate measurement of points. The automated measuring systems set up by image matching algorithms are still based on the point-to-point correspondence. However, linear feature contains more geometric and semantic information than point. It is also easier to be extracted from the photogrammetric images. Since the last decade, scholars and experts have been exploring the methods that linear feature takes place of point for solving photogrammetric problems (Schenk *et al.*, 1991, Li and Zhou, 1994). The researches show that linear features can be used to determine image orientation by space resection (Petsa and Patias, 1995, van den Heuvel, 1997, Kerschner, 1998, Hrabacek

and van den Heuvel, 2000, Smith and Park, 2000), or to measure object by model-image fitting (Vosselman and Haralick, 1996, van den Heuvel, 1999, van den Heuvel, 2000, Heuel and Förstner, 2001, Zhou and Li, 2001). These innovative researches lead the photogrammetric technology to a new stage which is called "*Line Photogrammetry*".

Although the CAD system is not initially developed for photogrammetric purpose, its powerful functions of drawing, manipulating, and visualizing 2D objects have made it being widely used with photogrammetric systems. The increasing demands of object's 3D models encourage many researches toward using 3D CAD models as a modelling tool to extracting objects from image data (Das *et al.*, 1997, Ermes *et al.*, 1999, Boehm *et al.*, 2000, van den Heuvel, 2000, Tseng and Wang, 2002). This trend towards integration of photogrammetry and CAD system in the algorithmic aspect creates a new term: "*CAD-based Photogrammetry*". Researches show that using CAD models does increase the efficiency of photogrammetric modelling by two reasons: (1) the advanced object modelling techniques such as Constructive Solid Geometry (CSG), (2) the incorporation of geometric object constraints.

Inspired by the line photogrammetry and CAD-based photogrammetry, we proposed a naval measuring tool – *floating model* – in this paper. The floating model represents a flexible entity floating in the 3D space. It can be a point, a line segment, a surface plane, or a volumetric model. Each model is associated with a set of shape parameters and a set of pose parameters. The pose parameters determine the datum point's position and the rotation of the model. The shape parameters

change the volume and the outline of the model. From the traditional photogrammetric point of view, the floating model is an extension of the floating mark. Instead, it is not only floated in the object space, but also deformable to fit the outline of the object. From the model-based building extraction point of view, floating mark is an exceptional case of floating model without any shape parameter. The details of floating models are given in the next chapter.

Comparing to other modelling schemes, such as polyhedral models, prismatic models, or parameterized polyhedral models, CSG models scheme do not use one complicated model for a whole building, but a combination of several volumetric primitives. A primitive is a predefined simple solid model which is associated with a number of parameters representing the shape and pose. The final complete model is composed of a number of primitives, following the Boolean set operation. These characteristics make CSG models flexible enough for modelling most of the buildings, yet still can be simply described by a small set of rules. Therefore, CSG modeling scheme is suggested for model-based building extraction by many pioneers (Braun *et al.*, 1995, Gülch *et al.*, 1998, Veldhuis, 1998, Ermes *et al.*, 1999, Tangelder *et al.*, 1999). The proposed floating model idea complies with the CSG principle. Each kind of floating models is a primitive. A building may be modelled by a combination of various floating models.

Model-based building extraction (Sester and Förstner, 1989, Vosselman, 1998, Brenner, 1999, Fischer *et al.*, 1999, Ameri, 2000, Suveg and Vosselman, 2000, Tseng and Wang, 2003) starts with hypotheses of building model representing a specified target on the scene, and verifies the compatibility between the model and the existing image data. Approaches to model-based building extraction are mostly implemented in a semi-automatic manner, solving the model-image fitting problem based on some high-level information given by the operator. The spatial data of a building object are determined, when model-image fitting is achieved optimally. Therefore, the key is the algorithm that is able to determine the pose and shape parameters of a floating model such that the edge lines of the wire-frame, as projected into the images, are optimally coincided with the corresponding edge pixels. It is assumed that the image orientations are known and the pose and shape parameters are approximately determined through an interactive process. To deal with this problem, we proposed a tailored least-squares model-image fitting algorithm in chapter 3 as a major component of the building extraction framework.

The proposed semi-automated strategy is shown as figure 1. The basic idea is based on "Human is good at interpretation, computer is good at calculation." Therefore, the high-level tasks, such as primitive selection, approximately fitting, Boolean set operation, and local modification, are accomplished by operator. While the low-level task, such as complicated calculation of optimally fitting, is accomplished by computer programs.
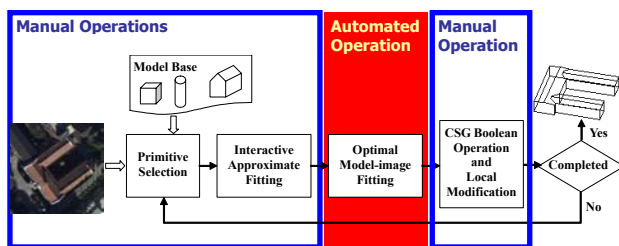

Figure 1. The proposed semi-automated strategy for model-based building extraction.

To test the practicability and to evaluate the accuracy, we designed a computer program for implementing the proposed procedures. Ten various buildings around the NCKU campus within four overlapped aerial images were selected as the experimental objects. Results and accuracy assessment are given in chapter 4, which shows the practical capability and potential.

2. BUILDING MODELLING

Building modelling and model-image fitting are two major issues in model-based building extraction. The issue on building modelling is how to establish a set of representative and complete building models. Buildings in Taiwan are highly diverse in appearance. It is almost impossible to categorize them into distinct styles of representative models. However, there is still regularity inherent in the most building structure, which allows describing buildings with a small set of rules. Since the buildings are basically volumetric objects, it is adequate to modelling by 3D solid entities. By summarizing the experiences of measuring by floating mark and reviewing the references of line photogrammetry and CAD-based photogrammetry, a naval measuring tool of "floating model" is proposed.

2.1 Floating Models

Traditional photogrammetric mapping systems concentrate on the accurate measurement of points. The floating mark is a simple way to represent the position of a point in the space, and thus, has been served as the only measuring tool on the stereo plotters up to nowadays. The idea behinds the floating mark is to depict the intersection V_1 of the bundle from the projection centers O_1 and O_2, through the image point v_1' and v_1'' to the ground, as figure 2 shows. If the conjugate point v_1' or v_1'' moves along the epipolar line, the intersection point V_1 represented by floating mark will raise or sink along the bundle, seems like "floating" in the object space. This simple representation of a 3D coordinates has been very useful for photogrammetric measurement and 2.5D mapping system. However, the floating mark reaches its limits when the conjugate points can not be identified due to the occlusions or interferences from other noises. And with the increasing needs of 3D object models, point-by-point measurement has been become the bottleneck of the production.
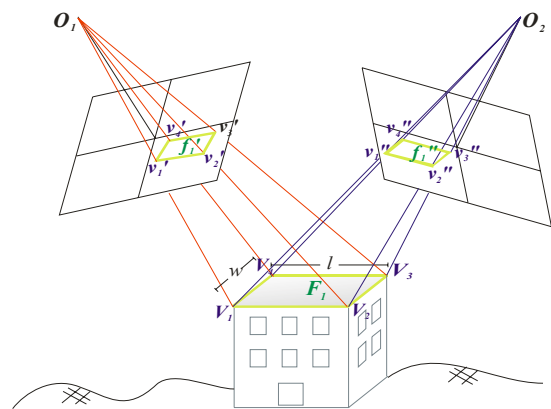

Figure 2. The concept of floating model.

Line photogrammetry takes the nature of 3D linear feature into consideration and introduces the 3D line equations as unknowns instead of 3D coordinates. Take figure 2 for example, operator

only has to measure any two points along $\overline{v_1'v_2'}$ on one image and any two points along $v_1''v_2''$ on the other image, then the line equations could be determined. The greatest benefit of line photogrammetry is avoiding the point identification and correspondence problem. Similar to the points, linear features can be used for solving intersection or resection problems. If the image orientation has been known, measuring linear features on the images can be used to extract 3D line segments. If the 3D line equations have been known, measuring linear features on the images can be used to determine image orientation.

The next development based on line photogrammetry is the CAD-based photogrammetry which is incorporated with various existing CAD models, such as box, cylinder, wedge, *etc*. The object model can be extracted by projecting wire-frame of CAD model onto the image and verifying the coincidence. The CAD-based photogrammetry has been successfully applied in some close-range photogrammetric applications, such as extracting oil pipes at an industrial plant. However, buildings are not so regular as industrial components. CAD models are not flexible enough to handle various kinds of building.

To deal with the modelling problem, we proposed a naval concept of floating models which complies with the constructive solid geometry. The floating model is basically a primitive CSG model, which determines the intrinsic geometric property of a part of building. The floating models can be categorized into four types: point, linear feature, plane, or volumetric solid. Each type contains various primitive models for the practical needs. For example, the linear feature includes the line segment and the arc. The plane includes the rectangle, the circle, the ellipse, the triangle, the pentagon, *etc*. The volumetric solid includes the box, the gable-roof house, the cylinder, the cone, *etc*. Despite the variety in their shape, each primitive model commonly has a datum point, and is associated with a set of pose parameters and a set of shape parameters. The datum point and the pose parameter determine the position of the floating model in object space. It is adequate to use 3 translation parameters (dX, dY, dZ) to represent the position and 3 rotation parameters, tilt (t) around Y-axis, swing (s) around X-axis, and azimuth (α) around Z-axis to represent the rotation of a primitive model. Figure 3 shows four examples from each type of models with the change of the pose parameters. X'-Y'-Z' coordinate system defines the model space and X-Y-Z coordinate system defines the object space. The little pink sphere indicates the datum point of the model. The yellow primitive model is in the original position and pose, while the grey model depicts the position and pose after changing pose parameters (dX, dY, dZ, t, s, α). It is very clear that, the model is "floating" in the space by controlling these pose parameters. The volume and shape of the model remain the same while the pose parameters change. The shape parameters describe the shape and size of the primitive model, e.g., a box has three shape parameters: width (w), length (l), and height (h). Changing the values of shape parameters elongates the primitive in the three dimensions, but still keeps its shape as a rectangular box. Various primitive may be associated with different shape parameters, e.g., a gable-roof house primitive has an additional shape parameter – roof's height (rh). Figure 4 shows three examples from each type of models with the change of shape parameters. The point is an exceptional case that does not have any shape parameters. The yellow one is the original model, while the grey one is the model after changing the shape parameters. The figure points out the other important characteristic of the floating model – the flexible shape with

certain constraints. Changing the shape parameters does not affect the position or the pose of the model.
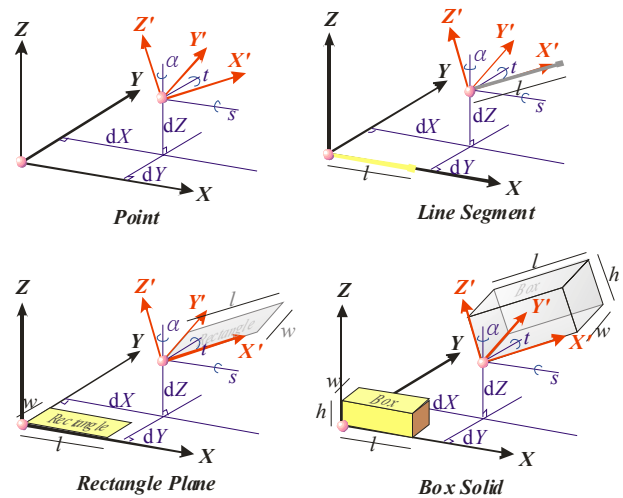

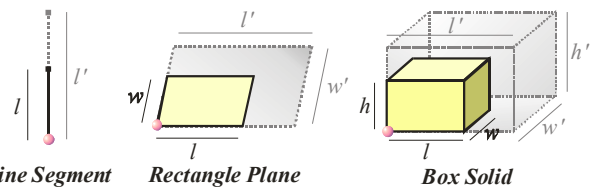Figure 3. Change the pose of floating models by adjusting pose parameters.

Figure 4. Change the shape of floating models by adjusting shape parameters.

2.2 CSG tree and Boolean Set Operation

The greatest benefit of constructive solid geometry is the flexibility of modelling complex buildings. In this paper, building parts are extracted by floating models one-by-one, then combined into a complete building model via Boolean set operations, such as union($\cup$), intersection($\cap$), and difference($-$). Figure 5 depicts the composition process of a complex building model, which is also called a CSG tree. The union operation may be the most commonly used. Since the building parts are extracted independently, discrepancy between connected walls is unavoidable. Special constraints or local modification should be provided to assisting the attaching process.
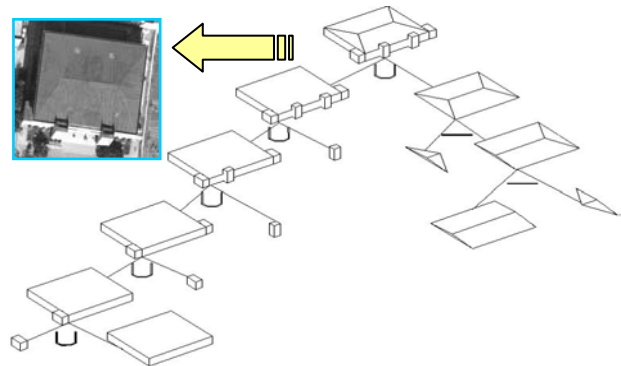

Figure 5. The CSG tree of a complex building model.

3. LEAST-SQUARES MODEL-IMAGE FITTING

The principle of model-image fitting algorithm is to adjust the shape and pose parameters of a primitive model, so it can fit the corresponding features extracted from the images. Since the floating model can be taken as a wire-frame model, the features for fitting are edge pixels. The optimal fit is achieved by minimizing the sum of the perpendicular distances from the edge pixels to the corresponding projected line of the wire-frame model. Figure 6 depicts the optimal fitting procedure. A model base which is a collection of various floating models has been pre-established. The selected primitive model is projected onto the image and fit the extracted edge pixels.
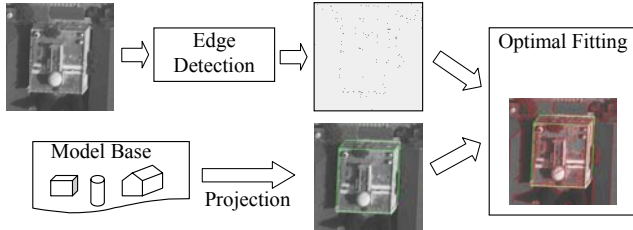

Figure 6. The procedures of optimal fitting.

3.1 Coordinate Systems

The proposed LSMIF algorithm performs the fitting in the photo coordinate system. A primitive model, however, is defined in the model space. It is necessary to transform a primitive model from model space to object space by introducing a set of shape and pose parameters. Then, it has to be projected onto the photo coordinate system with the known exterior orientation parameters. On the other hand, edge pixels extracted from the images should be transformed to the photo coordinate system for matching. Figure 7 shows the transformation of a box from model to photo coordinate system and the edge pixels from image to photo coordinate system.
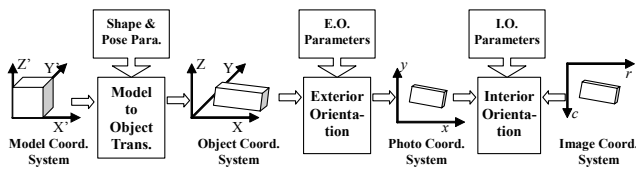

Figure 7. The coordinate systems involved with LSMIF.

The primitive model defined in the model space is a simple unit solid, e.g. a box is a unit cube of which width, length, and height are all equal to 1. The shape parameters will elongate or shorten the box to the correct size, and the pose parameters will rotate and move the box to the correct altitude and position in the object space. Table 1 lists the eight vertices coordinates transforming from model space to object space. Each vertex in the object space is then projected onto the images by the collinearity condition equations with the known exterior orientation elements

3.2 Approximate Fitting and Buffer

An approximate fitting is required before applying the LSMIF algorithm. An interactive program is developed for model selection, approximate fitting, and visualization. To obtain as close as to the right fitting, this program provides a user interface that allows the operator to resize, rotate, and move a model to fit the corresponding building images approximately. Benefited from the approximate fitting, the LSMIF iteratively pulls the model to the optimal fit instead of blindly searching for the solution. To avoid the disturbance of irrelevant edge pixels, only those edge pixels distributed within the specified buffer zones will be used in the calculation of the fitting algorithm. Figure 8 depicts the extracted edge pixels T_{ijk} and the buffer determined by a projected edge $\overline{v_{i1}v_{i2}}$ of the model. The suffix i represents the index of edge line, j represents the index of overlapped image, and k represents the index of the edge pixel. Filtering edge pixels with buffer is reasonable, because the discrepancies between the projected edges and the corresponding edge pixels should be small, as the model parameters are known approximately. However, the buffer size has to be carefully chosen because it will directly affect the convergence of the computation, i.e., the pull-in range.
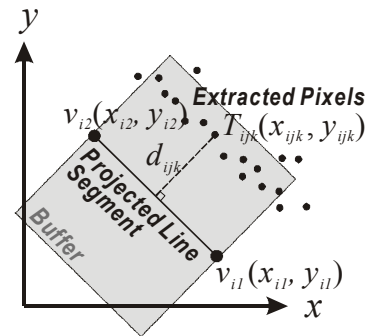

Figure 8. The extracted edge pixels and the buffer.

3.3 Objective Function and Least-squares Adjustment

That the fitting condition we are looking for is the projected model edge line exactly falls on the building edges in the images. In Eq.(1), the distance d_{ijk} represents a discrepancy between an edge pixel T_{ijk} and its corresponding edge line $\overline{v_{i1}v_{i2}}$, which is expected to be zero. Therefore, the objective of the fitting function is to minimize the squares sum of d_{ijk}. Suppose a projected edge line is composed of the projected vertices $v_{i1}(x_{i1}, y_{i1})$ and $v_{i2}(x_{i2}, y_{i2})$, and there is an edge pixel $T_{ijk}(x_{ijk}, y_{ijk})$ located inside the buffer. The distance d_{ijk} from the point T_{ijk} to the edge $\overline{v_{i1}v_{i2}}$ can be formulated as the following equation:

Table 1. Vertices coordinates from model space to object space.

Vertex No.	Model Space Coordinate	Multiply Shape Parameters	After Rotation	After Translation (Object Space Coordinate)
v_1	(0, 0, 0)	(0, 0, 0)	(0, 0, 0)	(dX, dY, dZ)
v_2	(1, 0, 0)	(w, 0, 0)	($w$cosα, $w$sinα, 0)	($w$cosα+dX, $w$sinα+dY, dZ)
v_3	(1, 1, 0)	(w, l, 0)	($w$cosα-$l$sinα, $w$sinα+$l$cosα, 0)	($w$cosα-$l$sinα+dX, $w$sinα+$l$cosα+dY, dZ)
v_4	(0, 1, 0)	(0, l, 0)	(-$l$sinα, $l$cosα, 0)	(-$l$sinα+dX, $l$cosα+dY, dZ)
v_5	(0, 0, 1)	(0, 0, h)	(0, 0, h)	(dX, dY, h+dZ)
v_6	(1, 0, 1)	(w, 0, h)	($w$cosα, $w$sinα, h)	($w$cosα+dX, $w$sinα+dY, h+dZ)
v_7	(1, 1, 1)	(w, l, h)	($w$cosα-$l$sinα, $w$sinα+$l$cosα, h)	($w$cosα-$l$sinα+dX, $w$sinα+$l$cosα+dY, h+dZ)
v_8	(0, 1, 1)	(0, l, h)	(-$l$sinα, $l$cosα, h)	(-$l$sinα+dX, $l$cosα+dY, h+dZ)

$$d_{ijk} = \frac{\left|(y_{ij1} - y_{ij2})x_{jk} + (x_{ij2} - x_{ij1})y_{jk} + (y_{ij2}x_{ij1} - y_{ij1}x_{ij2})\right|}{\sqrt{(x_{ij1} - x_{ij2})^2 + (y_{ij1} - y_{ij2})^2}} \quad (1)$$

where i = the index of the edge line
   j = the index of the overlapped image
   k = the index of the edge pixel

The photo coordinates $v_{i1}(x_{i1}, y_{i1})$ and $v_{i2}(x_{i2}, y_{i2})$ are functions of the unknown model parameters, comparatively the exterior-orientation parameters of photos are known. Therefore, d_{ijk} will be a function of the model parameters. Taking a box model for instance, d_{ijk} will be a function of w, l, h, α, dX, dY, and dZ, with the hypothesis that a normal building rarely has a tilt angle (t) or swing angle (s). The least-squares solution for the unknown parameters can be expressed as:

$$\Sigma\,d_{ijk}^2 = \Sigma\,[F_{ijk}(\,w,\,l,\,h,\,\alpha\,,\,\mathrm{d}X,\,\mathrm{d}Y,\,\mathrm{d}Z)]^2 \;\to min. \quad (2)$$

Eq.(2) is a nonlinear function with regard to the unknowns, so that the Newton's method is applied to solve for the unknowns. The nonlinear function is differentiated with respect to the unknowns and becomes a linear function with regard to the increments of the unknowns as follows:

$$d_{ijk} - F_{ijk0} = \left(\frac{\partial F_{ijk}}{\partial w}\right)_0 \Delta w + \left(\frac{\partial F_{ijk}}{\partial l}\right)_0 \Delta l + \left(\frac{\partial F_{ijk}}{\partial h}\right)_0 \Delta h + \left(\frac{\partial F_{ijk}}{\partial \alpha}\right)_0 \Delta\alpha +$$
$$\left(\frac{\partial F_{ijk}}{\partial dX}\right)_0 \Delta dX + \left(\frac{\partial F_{ijk}}{\partial dY}\right)_0 \Delta dY + \left(\frac{\partial F_{ijk}}{\partial dZ}\right)_0 \Delta dZ \quad (3)$$

in which, F_{ijk0} is the approximation of the function F_{ijk} calculated with given approximations of the unknown parameters. Given a set of unknown approximations, the least-squares solution for the unknown increments can be obtained, and the approximations are updated by the increments. Repeating this calculation, the unknown parameters can be solved iteratively.

The linearized equations can be expressed as a matrix form: $V=AX-L$, where A is the matrix of partial derivatives; X is the vector of the increments; L is the vector of approximations; and V is the vector of residuals. The objective function actually can be expressed as $q=V^TV \to min$. For each iteration, X can be solved by the matrix operation: $X=(A^TA)^{-1}A^TL$. The iteration normally will converge to the correct answer. However, inadequate relevant image features, affected by irrelevant features or noise, or given bad initial approximations may lead the computation to a wrong answer.

4. EXPERIMENTS

The test data are aerial photos of the NCKU campus, digitized by the photogrammetric scanner in $25\mu m$ resolution. The original photos are taken with a 305.11mm-focal-length aerial camera in the height about 1600m, so the average photo scale is about 1:5000. The end-lap between photos is more than 60%, and the side-lap is more than 30%. In the tests, buildings were extracted from the stereo image pairs formed by end-lap. Ten various buildings were arbitrarily selected for the test. All of the buildings are properly represented by a combination of box and gable-roof primitives, totally 23 primitives. For each primitive model, it takes about 20 sec to complete the fitting. Figure 9 shows an example of the fitting results. To evaluate the accuracy of LSMIF, all of the visible building corners were also measured by an experienced operator with an analytical plotter. Table 2 lists the average and RMS differences.

Table 2. The average and RMS differences of the building corner coordinates derived from LSMIF and manual measurements.

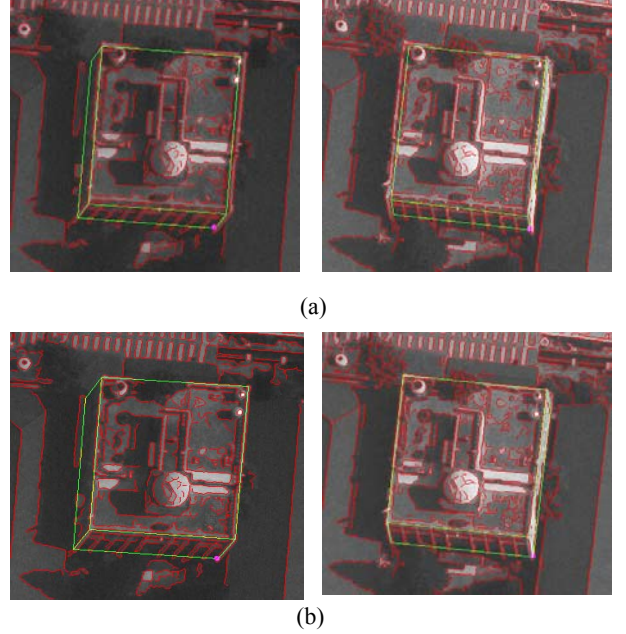|	$X(m)$	$Y(m)$	$Z(m)$
Average Diff.	0.161	0.007	0.047
RMS Diff.	0.330	0.277	1.034

(a)

(b)

Figure 9. (a) The image pair superimposed with the extracted edge pixels (red) and the projected wire-frame model (green) after manual approximate fitting. (b) The fitting result.

5. CONSLUSIONS

The objective of this study is to provide a semi-automated model-based building extraction system which can improve the efficiency of extracting and modelling buildings from multiple photogrammetric images. There are a number of characteristics of the proposed approach:

● The semi-automated strategy combines human ability on image interpretation and computer algorithmic potential.
● Compare to the traditional point-by-point mapping system, this approach provide floating models to extract data object-by-object.
● It is able to handle multiple images simultaneously, even combines aerial and close-range images.
● There is no need for stereo viewing.
● It complies with the constructive solid geometry, so the complex building can be modelled by a number of primitives.

The experiments results have shown the reliability and potential of this approach. If introducing adequate constraints, the influence from irrelevant noise data can be decreased and the accuracy will be improved. Besides, the floating models are not only capable of extracting buildings, but also capable of determining image orientation. The ideal scenario would be integrating the aerial and close-range photogrammetry. First,

extract the essential models of the building from orientation-known aerial images. Then, use these models to determine the orientation of the close-range images. Finally, extract the sophisticated model from close-range images.

6. REFERENCES

Ameri, B., 2000. Feature Based Model Verification (FBMV): A New Concept for Hypothesis Validation in Building Reconstruction, *International Archives of Photogrammetry and Remote Sensing*, Amsterdam, Vol. XXXIII, pp. 24-35.

Boehm, J., C. Brenner, J. Guehring and D. Fritsch, 2000. Automated Extraction of Features from CAD Models for 3D Object Recognition, *International Archives of Photogrammetry and Remote Sensing*, Amsterdam, Vol. XXXIII, pp. 76-83.

Braun, C., T.H. Kolbe, F. Lang, W. Schickler, V. Steinhage, A.B. Cremers, W. Förstner and L. Plumer, 1995. Models for Photogrammetric Building Reconstruction, *Computers & Graphics*, 19(1), pp. 109-118.

Brenner, C., 1999. Interactive Modelling Tools for 3D Building Reconstruction, *Photogrammetric Week '99*, Stuttgart, Vol. 47, pp. 23-34.

Das, S., B. Bhanu and C.-C. Ho, 1997. Generic Object Recognition Using CAD-Based Multiple Representations, *IEEE*, pp. 202-209.

Englert, R. and E. Gülch, 1996. One-eye Stereo System for the Acquisition of Complex 3D Building Descriptions, *GIS*, (4), pp. 1-11.

Ermes, P., F.A. van den Heuvel and G. Vosselman, 1999. A Photogrammetric Measurement Method Using CSG Models, *Proceedings of the ISPRS Workshop "Measurements Project Modeling and Documentation in architecture and Industry"*, Vol. XXXII, pp. 36-42.

Fischer, A., T.H. Kolbe and F. Lang, 1999. On The Use of Geometric and Semantic Models for Component-based Building Reconstruction, *Proceedings of Smati '99 Workshop*, Bonn, Vol. pp. 101-119.

Grün, A., 2000. Semi-automated Approaches to Site Recording and Modeling, *International Archives of Photogrammetry and Remote Sensing*, Amsterdam, Vol. XXXIII, pp. 309-318.

Gülch, E., H. Müller, T. Läbe and L. Ragia, 1998. On The Performance of Semi-automatic Building Extraction, *ISPRS Commission III Symposium on Object Recognition and Scene Classification from Multispectral and Multisensor Pixels*, Columbus.

Heuel, S. and W. Förstner, 2001. Matching, Reconstructing and Grouping 3D Lines from Multiple Views Using Uncertain Projective Geometry, *Proceedings of IEEE Computer Society Conference on Computer Vision and Pattern Recognition*, Hawaii, pp. 1-8.

Hrabacek, J. and F.A. van den Heuvel, 2000. Weighted Geometric Objects Constraints Integrated in a Line-Photogrammetric Bundle Adjustment, *International Archives of Photogrammetry and Remote Sensing*, Amsterdam, Vol. XXXIII, pp. 380-387.

Kerschner, M., 1998. Homologous Twin Snakes Integrated in a Bundle Block Adjustment, *ISPRS Commission III Symposium*, Columbus, Vol. XXXII, pp. 244-249.

Lang, F. and W. Förstner, 1996. 3D-City Modeling with a Digital One-eye Stereo System, *International Archives of Photogrammetry and Remote Sensing*, Vienna, Vol. XXXI, pp. 415-420.

Li, D. and G. Zhou, 1994. CAD-based Line Photogrammetry for Automatic Measurement and Reconstruction of Industrial Objects, *ISPRS Commission V Symposium on Close Range Techniques and Machine*, Melbourne, Vol. XXX, pp. 231-240.

Mohan, R. and R. Nevatia, 1989. Using Perceptual Organization to Extract 3-D Structures, *IEEE Transactions on Pattern Analysis and Machine Intelligence*, 11(11), pp. 1121-1139.

Petsa, E. and P. Patias, 1995. Straight Lines in Photogrammetry: Basic Algorithms, *Proceedings of Integrated Sensor Orientation*, Heidelberg, pp. 185-194.

Schenk, T., J.-C. Li and C. Toth, 1991. Towards an Autonomous System for Orienting Digital Stereopairs, *Photogrammetric Engineering & Remote Sensing*, 57(8), pp. 1057-1064.

Sester, M. and W. Foerstner, 1989. Object Location Based on Uncertain Models, *Mustererkennung 1989*, Springer Verlag, pp. 457-464.

Smith, M.J. and D.W.G. Park, 2000. Absolute and Exterior Orientation Using Linear Features, *International Archives of Photogrammetry and Remote Sensing*, Amsterdam, Vol. XXXIII, pp. 850-857.

Suveg, I. and G. Vosselman, 2000. 3D Reconstruction of Building Models, *International Archives of Photogrammetry and Remote Sensing*, Amsterdam, Vol. XXXIII, pp. 538-545.

Tangelder, J.W.H., P. Ermes, G. Vosselman and F.A. van den Heuvel, 1999. Measurement of Curved Objects Using Gradient Based Fitting and CSG Models, *International Archives of Photogrammetry and Remote Sensing*, Vol. XXXII, pp. 23-30.

Tseng, Y.-H. and S. Wang, 2002. Model-based 3D Reconstruction of Buildings from Multiple Aerial Images, *Geographic Information Sciences*, 8(1), pp. 16-23.

Tseng, Y.-H. and S. Wang, 2003. Semiautomated Building Extraction Based on CSG Model-Image Fitting, *Photogrammetric Engineering & Remote Sensing*, 69(2), pp. 171-180.

van den Heuvel, F.A., 1997. Exterior Orientation Using Coplanar Parallel Lines, *Proceedings of The 10th Scandinavian Conference on Image Analysis*, Lappeenranta, pp. 71-78.

van den Heuvel, F.A., 1999. A Line-Photogrammetric Mathematical Model for the Reconstruction of Polyhedral Objects, *SPIE*, Vol. 3641, pp. 60-71.

van den Heuvel, F.A., 2000. Trends in CAD-based Photogrammetric Measurement, *International Archives of Photogrammetry and Remote Sensing*, Amsterdam, Vol. XXXIII, pp. 852-863.

Veldhuis, H., 1998. Performance Analysis of Two Fitting Algorithms for the Measurement of Parameterised Objects, *International Archives of Photogrammetry and Remote Sensing*, Vol. XXXII, pp. 400-406.

Vosselman, G. and R.M. Haralick, 1996. Performance Analysis of Line and Circle Fitting in Digital Images, *Proceedings of The Workshop on Performance Characteristics of Vision Algorithms*, Cambridge, pp. 1-24.

Vosselman, G., 1998. Interactive Alignment of Parameterised Object Models to Images, *International Archives of Photogrammetry and Remote Sensing*, Columbus, Vol. XXXII, pp. 272-278.

Vosselman, G. and H. Veldhuis, 1999. Mapping by Dragging and Fitting of Wire-Frame Models, *Photogrammetric Engineering & Remote Sensing*, 65(7), pp. 769-776.

Zhou, G. and D. Li, 2001. CAD-Based Object Reconstruction Using Line Photogrammetry for Direct Interaction between GEMS and a Vision System, *Photogrammetric Engineering & Remote Sensing*, 67(1), pp. 107-116.

7. ACKNOWLEDGEMENTS